Dielectric Charging Effects in Electrostatically Actuated CMOS MEMS Resonators

Kristen L. Dorsey
Electrical and Computer Engineering
Carnegie Mellon University
Pittsburgh, USA
kristend@andrew.cmu.edu

Gary K. Fedder
Electrical and Computer Engineering and Robotics Institutes
Carnegie Mellon University
Pittsburgh, USA
fedder@ece.cmu.edu

Abstract—**Effects of dielectric charging on resonant frequency in an electrostatically actuated MEMS cantilever are experimentally observed over time and with changing bias voltage. Frequency sensitivity to bias of −11 Hz/V arises from non-linearity in the comb electrostatic force when the device is driven at 200 kHz oscillation. Frequency drift of greater than +200 ppm is observed over a 12 hr period when bias switches by more than 12 V. Borrowing from RF MEMS switch charging models, a device model is applied to the cantilever resonator oscillator system. These initial results inform design and compensation methods leading to decreased frequency drift and improved limit of detection for gravimetric sensing applications.**

I. Introduction

Electrostatically actuated CMOS MEMS resonators are well suited to chemical sensing due to their size and ease of integration with supporting circuitry. When functionalized with a sensitive layer, these resonators have applications as gravimetric sensors for sensing volatile organic compounds (VOCs) with a theoretical limit of detection (LOD) on the order of 10 femtograms [1]. In order to improve the limit of detection, factors that adversely affect frequency stability, e.g. drift, noise, and environmental conditions such as temperature and humidity, must be reduced or compensated.

Effects of charge injection into dielectric layers [2] have been observed in several electrostatically actuated MEMS devices containing oxide or nitride layers [2-9]. This behavior has been well characterized in RF MEMS switches, as it can severely impact device performance through reduction in pull-in voltage [3-5] or cause total failure through stiction [6]. While models have been created for RF switches, little work exists that shows the effects of dielectric charging on resonant structures, which also suffer degraded performance when subject to parasitic charging. Electrostatic spring softening effects giving rise to frequency drift of −200 to −300 ppm over 200 hours have been observed in oxidized silicon MEMS [7-8]. Due to the dielectric layers in the metal-oxide stack, CMOS MEMS resonators are particularly susceptible to dielectric charging.

Reduction or elimination of dielectric charge will lead to decreased frequency drift, increased stability, and improved limit of detection for sensed analytes. Design of highly linear capacitive designs is also expected to reduce drift. The particular cantilever resonators in this work exhibit a small non-linearity that, while deleterious for chemical sensing, is proving useful in understanding charging behavior in the CMOS MEMS technology. This paper examines the drift behavior of these cantilever resonators under various bias conditions to make progress toward an electromechanical model that includes charging effects and is extensible to predict behavior for future sensor design efforts.

II. Device Description

The MEMS device and on-chip electronics are fabricated in 0.35µm Bi-CMOS from TowerJazz Semiconductor. Structures are defined using the CMOS metal layers as a mask. The unmasked oxide is then etched to form the device from the CMOS back-end-of-line metal/dielectric stack. Subsequently the silicon is directionally etched and undercut to release the structure. An example device is shown in Fig. 1. After release, drops of polybutylmethacrylate (PBMA) are deposited into the target well and wicked into the cantilever beam, forming the chemically absorbent layer [10].

Fig. 2 provides the system schematic with the testbed. The resonator motion is sensed capacitively and the resultant signal is fed back to differential electrostatic actuators to create a free-running oscillator. The differential feedback signal ($\pm V_D$) of ±3.6 VAC is applied to the stator drive and a DC bias voltage (V_B) of 10-20 V is applied to the cantilever beam and sense and drive rotor fingers. The stator sense fingers attached to the inputs of the on-chip preamp, which have DC bias voltage of +2.4 V (V_{IO}).

The motional current output from the sense comb is detected by an on-chip voltage amplifier, phase shifted, and amplified by automatic gain control (AGC) circuitry.

NIOSH/CDC contract 200-2002-00528

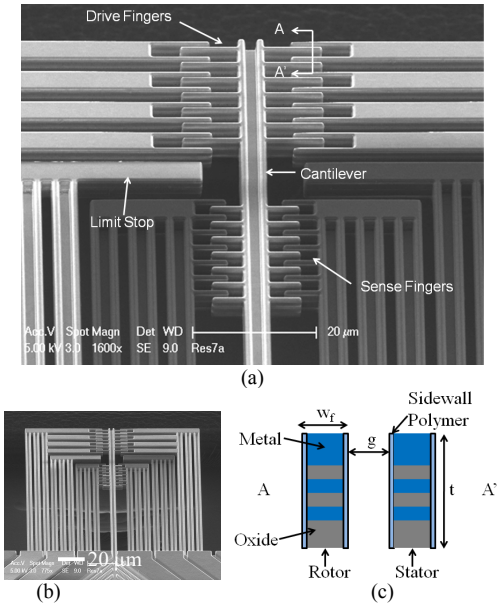

Figure 1: (a) An SEM image of a polymer filled cantilever resonator with length of 120 μm, width of 4 μm, finger width of 1 μm, thickness of 4.7 μm, finger gap of 0.8 μm, 7 sense fingers, and 7 drive fingers per side. (b) Full view of the resonator. (c) A-A' cross section of the rotor and stator fingers.

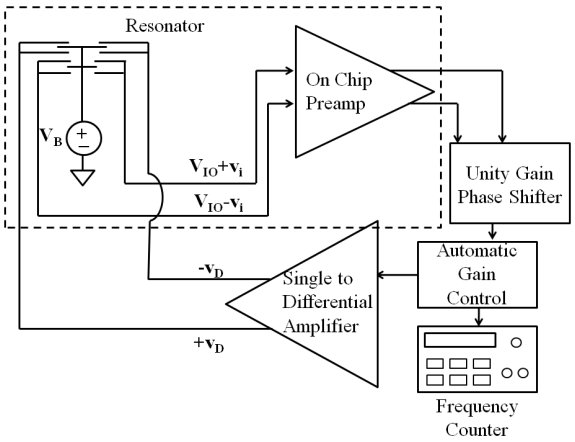

Figure 2: Block diagram of the oscillation circuitry. On-chip components are shown in the dotted box.

III. Modeling Device Behavior

A. Electrostatic Spring Softening

Due to the cantilever bending, the rotor comb fingers at the end of the cantilever do not form parallel-plate motion with respect to the stator fingers, and thus the capacitance is non-linear with displacement. While a first-order ideal lateral analytic model can be formed, it will not accurately account for fringing effects. Using Comsol Multiphysics finite element analysis (FEA) software, a model to determine the cantilever bending, capacitance with fringing fields, and degree of the non-linear component of electrostatic force was created. The model of cantilever bending is simplified to reduce computation time; only one sense finger and one drive finger on the rotor were included. In order to estimate the complete capacitance, the FEA results were multiplied by the number of comb fingers. Change in capacitance was calculated using a least squares fit to the model data and taking the derivative of the fit with respect to displacement.

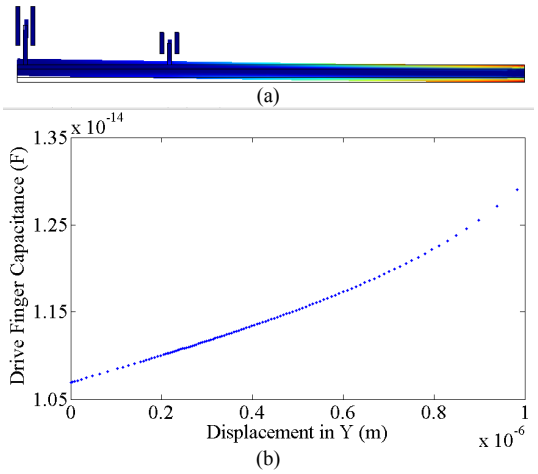

Figure 3: (a) FEA of beam bending in x and y during actuation. (b) Calculated capacitance with respect to displacement in y due to drive comb.

An example of the non-linear motion is presented in Fig. 3(a) and modeled capacitance is presented in Fig. 3(b). The gradient of the electrostatic force (*i.e.* the electrostatic spring softening factor) is

$$\frac{\partial F_e}{\partial x} = \frac{1}{2}\frac{\partial^2 C}{\partial x^2}V^2 = \gamma V^2 \qquad (1)$$

The FEA model predicts a spring softening coefficient of $\gamma_D = 9.32\times10^{-4}$ N/m/V^2 for the drive fingers and $\gamma_S = 1.93\times10^{-5}$ N/m/V^2 for the sense fingers, which is the modeled value averaged over the analytically estimated resonant displacement magnitude of 0.3 μm for $V_B = 13$ VDC to 0.7 μm for $V_B = 25$ VDC.

Using the values for γ_D and γ_S, the effect of bias voltage on resonant frequency can be estimated. As the DC voltage, V_{IO}, on the sense stator fingers due to the on-chip preamp input bias also contributes to the offset, the voltage across the sense fingers is $V_B - V_{IO}$. The resonant frequency with spring softening is

$$f = \frac{1}{2\pi}\sqrt{\frac{k_{mech} - \gamma_D\left(V_B^2 + \frac{V_D^2}{2}\right) - \gamma_S\left(V_B - V_{IO}\right)^2}{m_{eff}}} \qquad (2)$$

where k_{mech} is the mechanical spring constant, m_{eff} is the effective mass of the resonator, and V_D is the amplitude of the fed back drive waveform.

B. Surface Charge Behavior

In [7-8], dielectric surface charge in microstructures as the source of drift behavior is discussed. Fig. 4 is a simplified model of the CMOS MEMS air gap interface where both rotor and stator are uniformly coated with a dielectric sidewall polymer film.

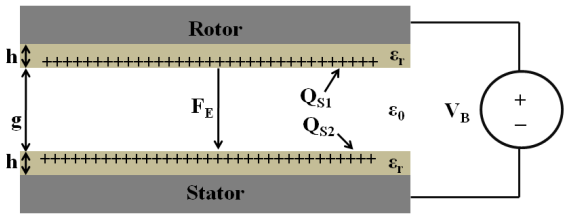

Figure 4: Simplified gap schematic with charging.

If a surface charge difference between fingers exists, a built-in voltage [7] will arise such that

$$\Delta V = \frac{h}{\varepsilon_0 \varepsilon_r}(Q_{S1} - Q_{S2}) \qquad (3)$$

where h is the thickness of the dielectric layer, ε_r is the relative permittivity of the dielectric film, and Q_{s1} and Q_{s2} are the time-varying dielectric surface charge. The resonant frequency is then found by substituting $V_B + \Delta V$ for V_B in (3), where ΔV is approximated as the same value for both sense and drive fingers.

IV. Results

In all experiments, the oscillator frequency from the AGC output is measured once per second using an Agilent 53132 universal frequency counter. Environmental factors, e.g. temperature and humidity, affect the resonant frequency of the sensor, and must be eliminated or compensated. The measured response of the cantilever oscillator to humidity is 0.4 Hz/%RH, which is substantial. In order to eliminate this response from the ambient, measurements were taken in a sealed testbed with a nitrogen flow of 1L/min. Surface temperature of the sensor package was also measured to compensate for temperature variations in the testbed. Measured temperature sensitivity is −35.5 Hz/°C.

A. Swept Bias Behavior

The PBMA filled sensor was placed in nitrogen flow for 12 hours in order to eliminate any residual water in the sensor or testbed. An initial bias voltage V_{B0} was held at +15 VDC for 12 hours. At the end of this period, oscillation frequency was recorded for a series of stepped V_B values. This experiment was repeated with two other initial bias values: 0 VDC and −15 VDC. The results are shown in Fig. 5.

The stepped bias voltage shows an electrostatic spring softening effect on resonant frequency with increased $|V_B|$ due to the non-linearity in the comb drive. Measurements for each bias step were manually recorded and took approximately 30 sec per step, leading to some frequency drift artifacts in Fig. 5.

In [9], charge injection into either the bottom electrode, coated with dielectric, or the top electrode, exposed to air, of an RF switch are discussed. Larger magnitude biases cause higher charge injection, decreasing bias voltage. A similar effect is observed in the resonator. The three initial bias conditions show a trend of increasing built-in voltage with increased held V_{B0} (Fig. 6) and a sensitivity of −0.079V/V. As the resonator is exposed to a positive bias, it is hypothesized that injected charge Q_{s2} increases, while for negative bias, injected charge Q_{s1} increases [2, 7, 9]. In either case, the built-in voltage decreases the effective bias voltage and increases the oscillation frequency of the resonator, as given in (2).

The γ values estimated by FEA predict a higher sensitivity to spring softening than measured, with a modeled sensitivity of −11.5 Hz/V and a measured sensitivity of −5.7 Hz/V. This difference may be due to errors in quantification of the height of the polymer and of material properties of the CMOS stack.

B. Stepped Bias Behavior

In this experiment, V_B was stepped from a grounded initial condition to a DC voltage and allowed to settle over several hours. Upon a step change in V_B, the resonator shows exponential response with time (Fig. 6). The frequency shift with time fits the equation

$$f(t) = A\exp(-t/\tau_1) + B\exp(-t/\tau_2) + f_0 \qquad (4)$$

where τ_1 and τ_2 are the time constants of the exponential step response, A and B are parameters that describe the magnitude of the drift, and f_0 is the oscillator frequency at t=0 when the voltage is initially stepped. The various tested bias conditions and subsequent time constant values are given in Table 1. The duration of the longer time constant (τ_2) increases with increasing stepped bias voltage.

In another experiment shown in Fig. 7, bias voltage was stepped twice: first from ground to an intermediate voltage (+20 V) and held for 5 min, then to a lower final voltage (−15 V). The resonator exhibits an increasing exponential step response between $t = 0$ and $t = 5$ min believed due to charge injection into the stator finger. At $t = 5$ min, the frequency instantaneously jumps by about 2500 ppm due to the decreased electrostatic softening arising from the smaller bias value. Then, a second exponential step response decreasing in frequency is observed for approximately 2 min. The cause of this decay is not known but thought to be discharge from the stator finger [9]. At $t = 10$ min, a third exponential response of increasing frequency is observed as stator charging occurs again. A frequency of 201.5 kHz is achieved in 8 hr, in comparison to the 12 hrs needed for settling in the single-step experiment of Fig. 6. These observations support our hypothesis that positive charge injection into the stator plate occurs. Beyond $t = 30$ min, what appears to be stochastic frequency drift is observed and may be due to flicker and random walk noise from charge states in the dielectric.

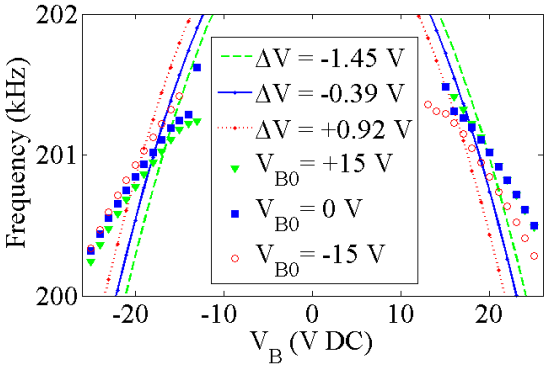

Figure 5: Effects of bias, V_B, on oscillation frequency for various initial bias states, V_{B0}, held for 12 hr. Frequency for −12 V < V_B < +12 V was not measured due to low loop gain.

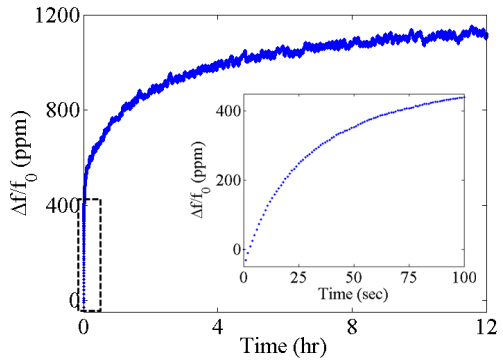

Figure 6: Frequency drift in a resonator upon +15 V bias step with jetted polymer. Inset figure shows frequency behavior for t = 0-100 sec. Frequency at t = 0 sec is 201.3 kHz. Frequency at t = 12 hr is 201.5 kHz

TABLE I. DRIFT TIME CONSTANTS IN POLYMER FILLED RESONATOR

V_{B0}	$V_{B\ Final}$	$\tau_{1\ (sec)}$	$\tau_{2\ (hr)}$
0 V	+13 V	71	2.77
0 V	+15 V	56	2.81
0 V	+20 V	76	3.96

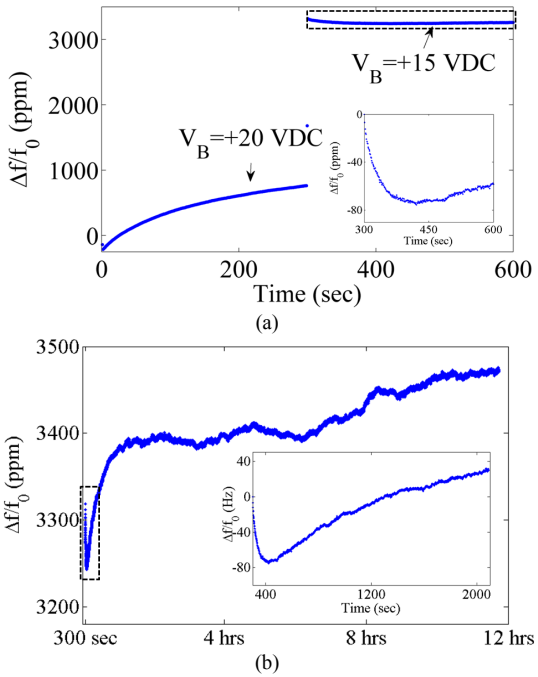

Figure 7: (a) Resonator response to stepped bias. Frequency at t = 0 sec is 200.8 kHz. Inset figure is response from t = 300 to t = 600 sec.
(b) Response of resonator after step to final value. Inset figure shows frequency drift from t = 300 sec to t = 2100 sec.

V. CONCLUSION

Due to its non-linear spring softening effect, the cantilever oscillator has proven to be a useful test structure to study the effects of dielectric charging on electrostatically actuated CMOS MEMS. Sensor behavior is highly dependent on external factors such as biasing, which change the dielectric charging of the resonator. Designs that have no geometric non-linearity in the electrostatic force should help eliminate the frequency drift phenomenon, even in the presence of charge drift. Bias methods to further reduce or eliminate surface charge will be explored in the future, as well as fabrication methods which may reduce resonator charging. Further study on the nature of rotor and stator charging is needed, in order to devise a model for dielectric charging applicable to electrostatically actuated resonators. This model may lead to design of more stable resonators and sensors with an increased limit of detection. Further tests on charging behavior are planned to refine the model for charge drift and help inform future design of CMOS MEMS resonators.

ACKNOWLEDGMENT

The authors would like to thank Suresh Santhanam for assistance with device fabrication.

REFERENCES

[1] S.S. Bedair and G.K. Fedder, "CMOS MEMS Microgroove Cantilever Oscillator Gas Vapor Sensor," presented at 12th Internation Meeting on Chemical Sensors, Columbus, USA, 2008.

[2] X. Yuan, C.M. Huang, D. Forehand, and C. Goldsmith, "Modeling and characterization of dielectric-charging effects in RF MEMS capacitive switches," in *2005 IEEE MTT-S International Microwave Symposium Digest*, 2005, pp. 753-756.

[3] G.N. Nielson and G. Barbastathis, "A physically based model for dielectric charging in an integrated optical MEMS wavelength selective switch," in *IEEE/LEOS International Conference on Optical MEMS and Their Applications*, 2005, pp.69-70.

[4] J. Wiebbeler, G. Pfeifer, and M. Hietschold, "Parasitic charging of dielectric surfaces in capacitive microelectromechanical systems," in *Sensors and Acutators A: Physical*, vol. 71, no. 1-2, pp. 74-80, Nov 1998.

[5] W.M. van Spengen, R. Puers, R. Mertens, and I. De Wolf, "A comprehensive model to predict the charging and reliability of capacitive RF MEMS switches," in *J. Micromech. Microeng.*, vol. 14, pp. 514-521, Jan 2004.

[6] R.W. Herft, P.G. Steeneken, H.G.A. Huizing, and J. Schmitz, "Chenter-shift method for the characterization of dielectric charging in RF MEMS capacitive switches," in *IEEE Trans. Semiconductor Manufacturing*, vol. 21, no. 2, pp. 148-153, May 2008.

[7] G. Bahl, "Model and observation of dielectric charge in thermally oxidized silicon resonators," in *J. MEMS*, vol. 19, no. 1, pp. 162-174, Feb 2010

[8] S. Kalicinski, H.A.C. Tilmans, M. Wevers, and I. De Wolf, "A new characterization method for electrostatically actuated resonant MEMS: Determination of the mechanical resonance frequency, quality factor and dielectric charging," in *Sensors and Actuators A: Physical*, vol. 154, no. 2, pp. 304-315, Sept 2009.

[9] Z. Peng, X. Yuan, J.C.M. Huang, D. Forehand, and C.L. Goldsmith, "Top vs. bottom charging of the dielectric in RF MEMS capacitive switches," in *Proceedings of the Asia-Pacific Microwave Conference*, 2006, pp. 1535-1539

[10] S.S. Bedair and G.K. Fedder, "Polymer mass loading of CMOS/MEMS microslot cantilever for gravimetric sensing," in *Proceedings of IEEE Sensors*, 2007, pp.1164-1167.